Am J Clin Exp Urol 2024;12(1):28-35
www.ajceu.us /ISSN:2330-1910/AJCEU0146950

Original Article

Prediction of Fuhrman pathological grade of renal clear cell carcinoma based on CT texture analysis

Zhuang Dong[1], Chao Guan[1], Xuezhen Yang[1,2]

[1]Department of Urology, The Second Affiliated Hospital of Bengbu Medical University, Bengbu 233020, Anhui, China; [2]Department of Urology, Qingdao West Coast New District People's Hospital, Shandong Second Medical University, Qingdao 266400, Shandong, China

Received October 11, 2022; Accepted January 10, 2024; Epub February 15, 2024; Published February 28, 2024

Abstract: Objective: To study the predictive performance of the imaging model based on the texture analysis of CT plain scan in distinguishing between low (grade I and II) and high (grade III and IV) of Fuhrman pathological grade of renal clear cell carcinoma. Methods: The clinical data of 94 patients with ccRCC who underwent CT scan and were confirmed by biopsy or surgery in TCGA-KIRC public database were retrospectively analyzed. There were 32 cases of low-grade ccRCC and 62 cases of high-grade ccRCC. The patients were randomly divided into training set and verification set according to the proportion of 7:3 by stratified sampling method. The imaging characteristics of ccRCC were calculated in the plain CT images. Lasso regression was used to reduce the dimensionality of the imaging characteristics of the training set, and binary logistic regression was used to construct the prediction model. Bootstrap method was used to verify the training set model and the validation set model, and the area under the receiver operating characteristic (ROC) curve (AUC) was calculated respectively. Results: Binary logistic regression showed that only imaging features were independent risk factors for predicting the Furhman classification of ccRCC. The predictive model was $y = 1/[1 + \exp(-z)]$, $z = 1.274 \times$ imaging risk score + 0.072. The results of bootstrap internal validation showed that the AUC of the training group was 0.961 (95% CI: 0.900-0.913). The Hosmer-Lemeshow goodness of fit test showed that the prediction model had a good calibration in the training group (P = 0.416). The AUC of prediction model in validation group was 0.731 (95% CI: 0.500-1.000). The Hosmer-Lemeshow goodness of fit test results showed that the prediction model had a good calibration in the validation group (P = 0.592). Conclusion: The model based on CT texture analysis has a good predictive effect in differentiating low-grade and high-grade ccRCC and can provide reference for the treatment and prognosis of patients.

Keywords: Renal clear cell carcinoma, texture analysis, radiomics, prediction model

Introduction

Renal cell carcinoma (RCC) accounts for about 85-90% of all renal malignant tumors [1, 2]. The most common types of renal cell carcinoma are clear cell carcinoma (ccRCC), papillary cell carcinoma (PRCC) and chromophobe cell carcinoma (CRCC) [3]. Renal clear cell carcinoma is the main type, accounting for about 70% of all cases. Compared with PRCC and CRCC, the survival rate of ccRCC is lower than 5 years, and the transfer risk is higher [4]. Therefore, tumor staging and grading is one of the important tasks of tumor diagnosis and treatment. Tumor grading defines the differentiation of tumor cells relative to normal cells. It is an indicator of tumor growth and diffusion rate. The Fuhrman nuclear grading system is the most widely used grading system at present, and it is also an independent predictor of tumor invasion and patient prognosis [5]. It is based on the evaluation of the following nuclear characteristics: the size of the nucleus, the shape of the nucleus, and the prominence of the nucleolus. Based on these assessments, tumors will be classified into four different levels (I-IV). Grade I and Grade II are considered as low-grade tumors with good prognosis, while Grade III and Grade IV are considered as high-grade tumors with poor prognosis [6]. At present, fine needle aspiration and image-guided biopsy are the gold standard for preoperative renal tumor grading. However, due to the heterogeneity of tumors, these technologies have defects such

https://doi.org/10.62347/GUWV5636

as infection, hemorrhage, tumor cell proliferation, and cannot provide information about the entire tumor. Because of the intratumoral heterogeneity of ccRCC, biopsy underestimated the Fuhrman grade in 55% of cases. In the past decade, many non-invasive treatment strategies for RCC have been designed, including radiofrequency ablation, cryoablation and active monitoring [7, 8]. However, most patients often undergo surgical treatment after diagnosis, so it is necessary to recommend individualized treatment strategies. Only invasive or high-level ccRCC tumors (III, IV) are treated with radical treatment (such as surgery), while low-grade (I, II) lesions are treated with conservative treatment (such as active monitoring) [9, 10]. It is necessary to develop an accurate and non-invasive preoperative Fuhrman grading method for renal cell carcinoma to guide the decision-making process. Previous studies have shown that the imaging features are valuable for distinguishing between high and low grade ccRCC tumors. To our knowledge, few studies have explored the value of CT plain scan texture analysis in predicting the nuclear grade of clear cell renal cell carcinoma. In this study, we aimed to evaluate the predictive performance of the model constructed based on CT texture analysis in differentiating low nuclear and high nuclear clear cell renal cancer, which can provide reference for the treatment and prognosis of patients.

Materials and methods

This study further established a model by extracting patient CT textual features and using statistical methods to predict the differentiation of high and low grade renal clear cell carcinoma. Retrospective analysis of clinical, histopathological and imaging data of 945 patients from TCGA-KIRC and cancer imaging archives from January 1, 1998 to December 31, 2013 [11, 12] (Ethical approval and informed consent were not obtained for this retrospective study, because all unidentified data of patients in this study have been published and used for scientific purposes for free). Inclusion criteria: 1. Both imaging data and clinical data are available; 2. Single lesion with clear ccRCC grading. Finally, 94 cases were included. Exclusion criteria: 1. Metastasis of cancer; 2. The thickness of non-enhanced CT before operation is higher than 5 mm; 3. Cystic manifestations; 4. He received treatment for renal cell carcinoma before plain CT scan; 5. Poor image quality. In this study, grade I and II are defined as low level ccRCC, and grade III and IV are defined as high level ccRCC, including 32 cases in low level group, 62 cases in high level group, 65 males and 29 females, aged 22-90 years, with an average age of (60.88 ± 13.85) years.

Image data parameters

CT acquisition parameters are as follows: slice thickness 5 mm; Tube voltage: 120-140 kv; Tube current: 95-575 mA; Pixel size is 0.562 × 0.562 mm^2 to 0.976 × 0.976 mm^2. TCGA-KIRC database includes various data sources. Therefore, in order to achieve a completely unified imaging standard, all images must go through some preprocessing steps to minimize the possible consequences caused by the heterogeneity of different standards.

Area of interest delineation

94 cases of CT plain scan images and enhanced CT images were imported into 3D Slicer v4.11.0 [13] software, and compared with enhanced CT images, the region of interest (ROI) can be delineated more accurately manually. It was completed by two radiologists with 5 years or more of work experience. First, one radiologist sketched the area of interest of renal cancer and saved it as a boundary file (.nrrd file format). After 1-2 months, another radiologist manually revised the boundary file [14] to ensure accuracy. In case of dispute, the two parties reached a consensus through consultation. ROI delineation principle: delineate ROI in layers within 1 mm from the inner side of the lesion edge (**Figure 1**).

Extracting omics features and modeling

Use PyRadiomics software (version 3.0.1) [15] to extract texture features from original images, filtered images and wavelet transform images. The Laplacian of Gaussian (LoG) filter is used to filter the image. The filter values are 2, 4 and 6 mm, respectively, representing fine, medium and rough patterns. We use PyWavelet (version 0.5.2) [16] to generate wavelet-based texture features. Wavelet transform is an image processing technology that uses a combination of high-frequency and low-frequency band-pass filters to decompose an image to obtain impor-

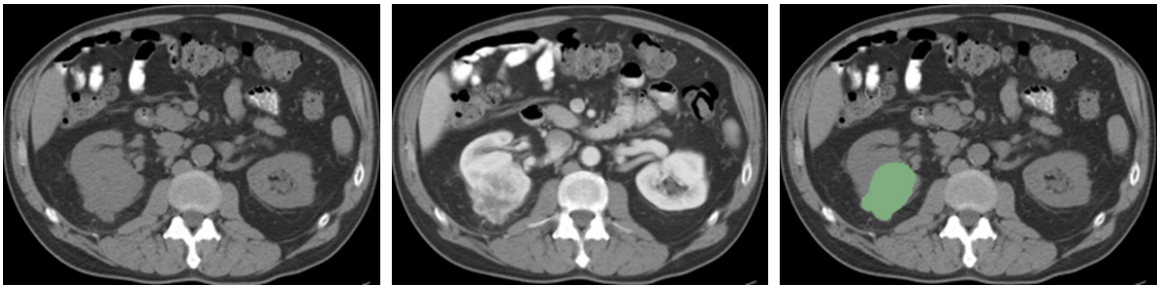

Figure 1. Delineation of ROI.

tant information that may be hidden from the image [17]. The omics features were extracted from the filtered image, and 107 features were obtained, including 19 histogram features, 16 3D morphological features, 10 2D morphological features, 22 gray level co-occurrence matrices, 16 gray level run distance matrices, 16 gray level area size matrices, 5 adjacent gray level difference matrices, and 14 gray level dependency matrices. The samples are divided into training sets and test sets by hierarchical sampling at a ratio of 7:3. In order to avoid dimensional disasters caused by too many features, the 107 features obtained are first screened by Lasso regression, which is applicable to high-dimensional data penalty estimation, and the alpha parameter with the lowest error is selected. Finally, 10 features are retained in the reduced dimension. Based on the final 10 features, a binary logistic regression model is established, the receiver characteristic operator (ROC) of the model is drawn, and the area under curve (AUC) of the ROC curve is calculated. Finally, decision curve analysis (DCA) was performed on the model to evaluate the pathological grade of renal clear cell carcinoma, and check model accuracy.

Statistical analysis

R v. x64 3.6.1 software was used for statistical analysis. The dimension reduction of the training set's image features adopted Lasso regression, which is suitable for penalty estimation of high-dimensional data. In clinical data analysis, chi square test was used for categorical variables, and the results were expressed in percentage (%); Rank sum test was used for rank variables, and the results were expressed in percentage (%); The numerical variables were tested by t test, and the results were expressed by mean (standard deviation). With Furhman grading as the diagnostic standard of ccRCC, the patient's clinical information, CT signs and iconographic scores as independent variables, and binary logistic regression was used to build a parametric prediction model. Bootstrap method was used to verify the model internally, and the area under the curve (AUC) of the ROC curve was calculated. The prediction model is used in the validation set data to calculate the AUC value. The calibration of the evaluation model was tested by Hosmer Lemeshow goodness of fit. The decision-making curve was used to analyze the patients' net benefits under different probability thresholds for the prediction model of the validation group's imageology. The difference was statistically significant with $P<0.05$.

Results

General information of low- and high-level patients in training group and validation group was shown in **Table 1**.

In the training group and validation group, the gender and age of low and high level ccRCC were not statistically significant ($P>0.05$), and TNM staging was statistically significant ($P<0.05$). After image preprocessing and feature extraction through the Pyronics toolkit, 107 basic omic features were screened. Finally, the LASSO regression method was used to reduce the dimensions and retain the 10 most significant omic features, as shown in **Table 2**.

A binary logistic regression model was established. According to the ROC curve of the model, the AUC of the training set was 0.961 (95% CI: 0.900-0.913), and the AUC of the validation set was 0.731 (95% CI: 0.500-1.000) (**Figure 2**).

According to the best model parameters, the final LR model is established using all training

Table 1. Comparison of general data between training group and validation group in patients with low and high grade renal clear cell carcinoma

Parameter	Training group			Test group		
	Low level (n = 23)	High level (n = 50)	*P* value	Low level (n = 9)	High level (n = 12)	*P* value
Gender (Female/Male, Cases)	7/16	24/36	1.000	4/5	4/8	0.948
Age (mean ± sd, Years)	59.83 (10.90)	61.02 (12.15)	0.689	62.67 (18.99)	60.00 (13.36)	0.709
TNM staging (%)			0.018			0.021
I	19 (82.6)	22 (44.0)		7 (77.8)	2 (16.7)	
II	1 (4.3)	3 (6.0)		0 (0.0)	2 (16.7)	
III	2 (8.7)	12 (24.0)		2 (22.2)	3 (25.0)	
IV	1 (4.3)	13 (26.0)		0 (0.0)	5 (41.7)	

Table 2. Lasso regression analysis results of imaging histological characteristics

Iconographic characteristics	Variables in the model
Original_shape features	Maximum 2D Diameter Slice
	Sphericity
Firstorder features	Minimum
	Range
Glcm features	MCC
	Idmn
Glszm features	Small Area Emphasis
Gldm features	Large Dependence LowGrayLevel Emphasis
	Dependence NonUniformity
Shape features	Least Axis Length

set data. The results of Hosmer-Lemeshow goodness of fit test show that the GiViTI calibration curve band of the prediction model in the training group and the verification group does not cross the 45° angle bisector in the 80% and 95% confidence interval regions (P>0.05), and the calibration of the prediction model in the training group and the verification group is good (**Figure 3**).

Finally, the clinical decision curve was established through machine learning (**Figure 4**). The results showed that when the probability threshold was 2-95%, the models of the training group and the verification group predicted that the patients' net benefits from ccRCC pathological grading were higher than those from all patients who were considered as high or low level, which could make the patients benefit from it.

Discussion

Renal cell carcinoma (RCC) is the most common type of renal cancer, accounting for about 2% of global cancer deaths. The 5-year survival rate of localized tumors was 93%, and the 5-year survival rates of lymph node metastasis and distant metastasis were 69% and 12%, respectively [18]. Among different histological subtypes, patients with clear cell RCC (ccRCC) have proved to have worse prognosis than other histological subtypes (pRCC and crRCC) [19]. However, according to the traditional CT film reading method, imaging physicians can only roughly evaluate the stage of renal clear cell carcinoma patients, and it is difficult to predict their Fuhrman grade. Nowadays, the application of texture analysis in medical images, especially in the field of tumor, has become a hot spot for many scholars.

This paper is a study on the prediction of pathological grading of ccRCC by plain CT texture analysis. The pathological grading of ccRCC is one of the most important factors affecting clinical decision-making. For low grade patients, active monitoring and partial nephrectomy can be carried out, while for high grade patients, radical nephrectomy, radiotherapy and chemotherapy can be selected. As far as we know, only a few studies have used CT texture analysis to predict the nuclear grade of RCC in clear cells [20, 21]. However, all studies were limited to the analysis of contrast-enhanced CT images (corticomedullary phase and renogram phase). Since the nuclear grade is not directly related to the evaluation of tumor vascular density under microscope, it is reasonable to use non enhanced CT. Therefore,

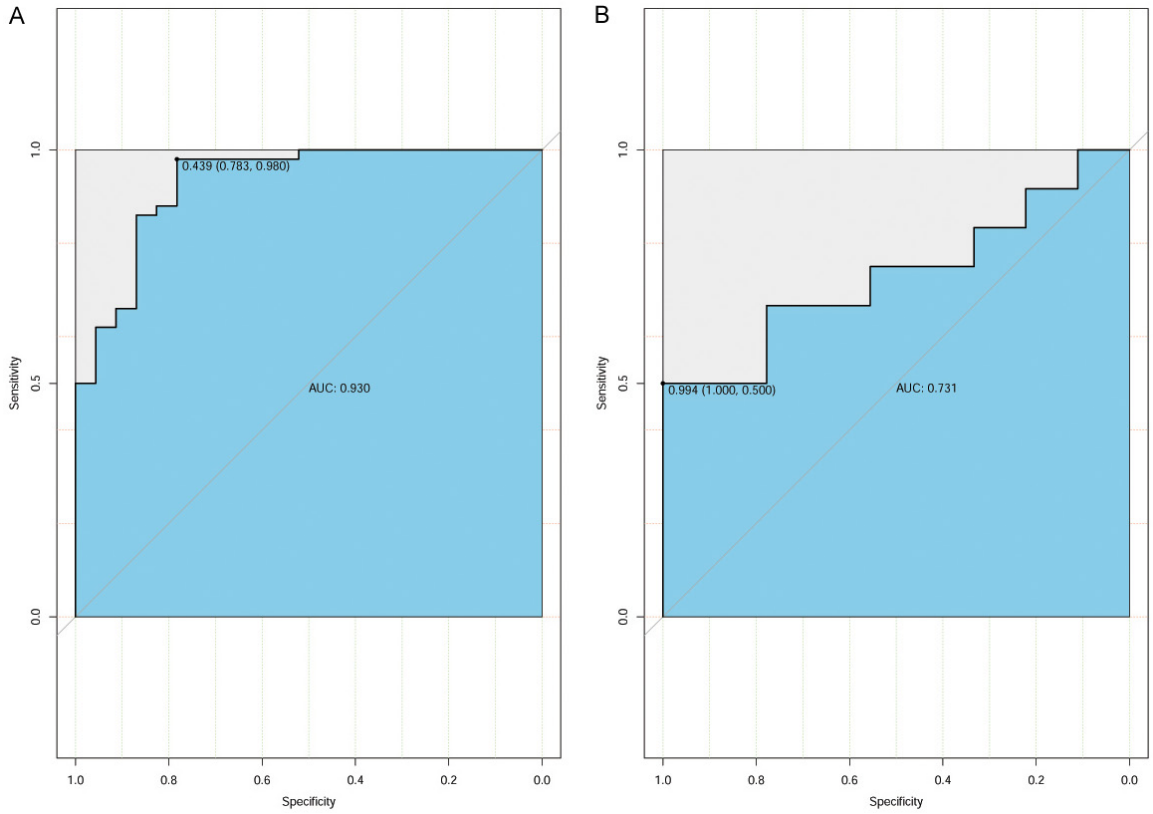

Figure 2. ROC curve of prediction model of training group and verification group. A. ROC curve of training group; B. ROC curve of validation group.

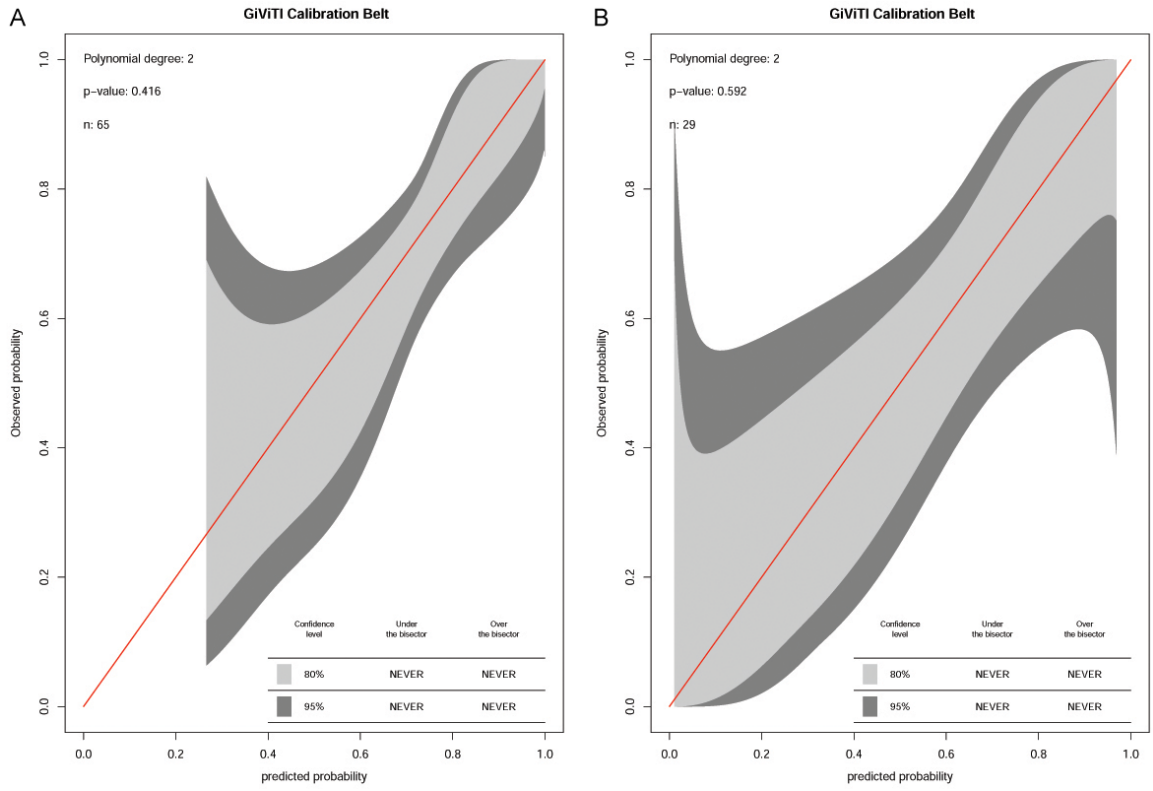

Figure 3. Correction curve of prediction model of training group and verification group. A. Calibration curve of training group; B. Calibration curve of validation group.

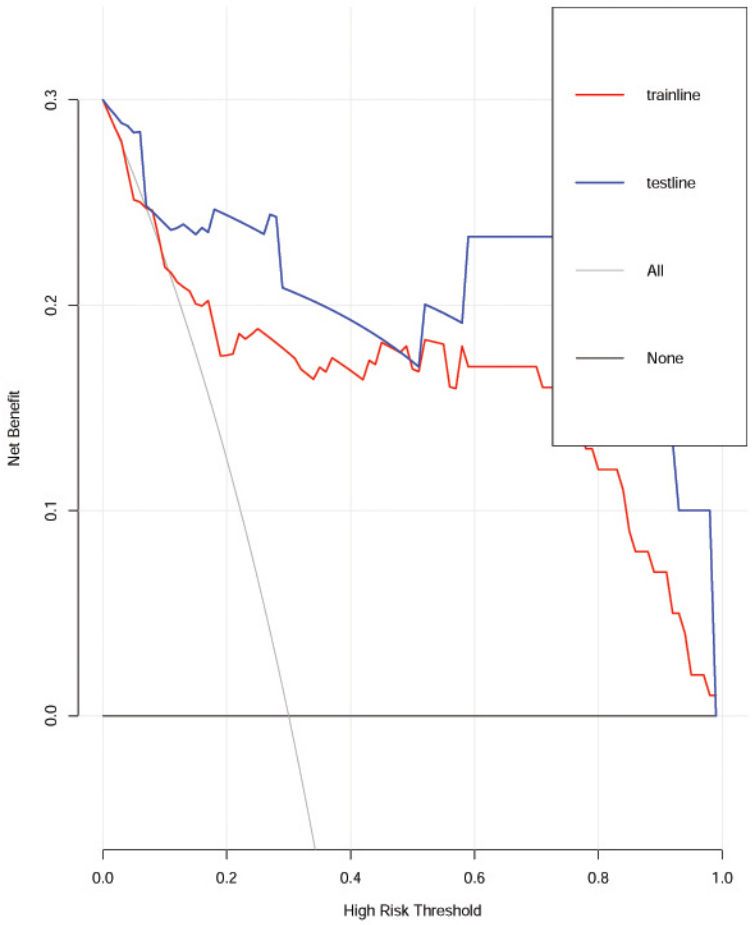

Figure 4. Clinical decision curve of predictive model in training group and validation group. Red is the training group; Blue is the validation group.

this study only used plain CT images for imaging analysis.

The Fuhrman nuclear grading system released in 1982 is the most widely used one, and it is also an independent predictor of tumor invasion and patient prognosis [22]. In this study, a simplified Fuhrman nuclear grading system was also used, which divided ccRCC into four grades. Grade I to II are low grade tumors with good prognosis, and grade III to IV are high grade tumors with poor prognosis [23, 24]. Texture analysis is a process of extracting texture feature parameters at the voxel or pixel level using certain image processing techniques to obtain quantitative or qualitative description of texture [25-27]. This method can generate a large number of features, making the technology have a high dimension.

In this study, plain CT texture analysis technology shows a high predictive ability in judging the pathological grading of ccRCC. It extracts texture features, and then further reduces data dimensions and establishes models. The feature dimension reduction adopts Lasso regression which is applicable to high-dimensional data, and the penalty term is added to its cost function to make the model correspond to a smoother function, so the model is simpler and not easy to produce over fitting. Cross validation is used to obtain the minimum cost function λ Value to make the test model closest to the ideal model. Automatic feature selection is realized, which makes the model easy to interpret. Subsequently, CT texture features, traditional imaging features and TNM staging were included in binary logistic regression. The results showed that only CT texture analysis was an independent risk factor for predicting the degree of differentiation of ccRCC, which achieved high differentiation and calibration in both the training group and the verification group. The AUC is slightly higher than the prediction model established by Kocak et al. [21] using texture features (AUC = 0.656, sensitivity and specificity are 75.3% and 53.5% respectively), but lower than the prediction model based on texture features reported by Ding et al. [28] (AUC = 0.780, 95% CI: 0.666-0.894). It may be that the model and scanning parameters used for sample collection in TCGA-KIRC database are inconsistent or the spatial dimension of this study is higher, which leads to the low AUC results of its validation set. The traditional imaging features and clinical data in this study did not enter the prediction model, which is consistent with the research results of Ding et al.

Shortcomings of this study: (1) In this retrospective study, the overall sample size is relatively small, and the sample distribution has some bias, which may lead to over fitting and non-fitting of classification. (2) When delineating VOI, the accuracy of delineating lesions is

reduced due to unclear edges of some masses or the influence of partial volume effect. (3) This study lacks external validation, and only uses a simple 10-fold cross validation method for logistic regression analysis to avoid too good results. (4) The image database of TCGA-KIRC in cancer image archives includes patients from different centers and sources with different image acquisition schemes. In order to minimize changes and impacts between scanners, all image datasets we studied have gone through some preprocessing steps before texture analysis, such as normalization, discretization and pixel re adjustment [29].

In conclusion, the prediction model based on plain CT texture analysis has a high diagnostic efficiency in predicting Furhman pathological grading of ccRCC patients and is a promising non-invasive diagnostic method.

Acknowledgements

We would like to express our gratitude to all of the people who helped during the writing of this manuscript, and to the peer reviewers for their constructive opinion and suggestions.

Disclosure of conflict of interest

None.

Address correspondence to: Chao Guan and Xuezhen Yang, Department of Urology, The Second Affiliated Hospital of Bengbu Medical University, Bengbu 233020, Anhui, China. E-mail: chaoguan666516@163.com (CG); engineyang@sina.com (XZY)

References

[1] Srigley JR, Delahunt B, Eble JN, Egevad L, Epstein JI, Grignon D, Hes O, Moch H, Montironi R, Tickoo SK, Zhou M and Argani P; ISUP Renal Tumor Panel. The International Society of Urological Pathology (ISUP) vancouver classification of renal neoplasia. Am J Surg Pathol 2013; 37: 1469-1489.

[2] Miller KD, Fidler-Benaoudia M, Keegan TH, Hipp HS, Jemal A and Siegel RL. Cancer statistics for adolescents and young adults, 2020. CA Cancer J Clin 2020; 70: 443-459.

[3] Kim JH. Re: Lorenzo Marconi, Saeed Dabestani, Thomas B. Lam, et al. Systematic review and meta-analysis of diagnostic accuracy of percutaneous renal tumour biopsy. Eur Urol 2016;69:660-73. Eur Urol 2016; 70: e139-e140.

[4] Delahunt B, Cheville JC, Martignoni G, Humphrey PA, Magi-Galluzzi C, McKenney J, Egevad L, Algaba F, Moch H, Grignon DJ, Montironi R and Srigley JR; Members of the ISUP Renal Tumor Panel. The International Society of Urological Pathology (ISUP) grading system for renal cell carcinoma and other prognostic parameters. Am J Surg Pathol 2013; 37: 1490-1504.

[5] Lohse CM, Blute ML, Zincke H, Weaver AL and Cheville JC. Comparison of standardized and nonstandardized nuclear grade of renal cell carcinoma to predict outcome among 2,042 patients. Am J Clin Pathol 2002; 118: 877-886.

[6] Delahunt B. Advances and controversies in grading and staging of renal cell carcinoma. Mod Pathol 2009; 22 Suppl 2: S24-36.

[7] Blumenfeld AJ, Guru K, Fuchs GJ and Kim HL. Percutaneous biopsy of renal cell carcinoma underestimates nuclear grade. Urology 2010; 76: 610-613.

[8] Tomaszewski JJ, Uzzo RG and Smaldone MC. Heterogeneity and renal mass biopsy: a review of its role and reliability. Cancer Biol Med 2014; 11: 162-172.

[9] Ljungberg B, Albiges L, Abu-Ghanem Y, Bensalah K, Dabestani S, Fernández-Pello S, Giles RH, Hofmann F, Hora M, Kuczyk MA, Kuusk T, Lam TB, Marconi L, Merseburger AS, Powles T, Staehler M, Tahbaz R, Volpe A and Bex A. European Association of Urology guidelines on renal cell carcinoma: the 2019 update. Eur Urol 2019; 75: 799-810.

[10] Yoon YE, Lee HH, Kim KH, Park SY, Moon HS, Lee SR, Hong YK, Park DS and Kim DK. Focal therapy versus robot-assisted partial nephrectomy in the management of clinical T1 renal masses: a systematic review and meta-analysis. Medicine (Baltimore) 2018; 97: e13102.

[11] Clark K, Vendt B, Smith K, Freymann J, Kirby J, Koppel P, Moore S, Phillips S, Maffitt D, Pringle M, Tarbox L and Prior F. The Cancer Imaging Archive (TCIA): maintaining and operating a public information repository. J Digit Imaging 2013; 26: 1045-1057.

[12] Shinagare AB, Vikram R, Jaffe C, Akin O, Kirby J, Huang E, Freymann J, Sainani NI, Sadow CA, Bathala TK, Rubin DL, Oto A, Heller MT, Surabhi VR, Katabathina V and Silverman SG. Radiogenomics of clear cell renal cell carcinoma: preliminary findings of The Cancer Genome Atlas-Renal Cell Carcinoma (TCGA-RCC) Imaging Research Group. Abdom Imaging 2015; 40: 1684-1692.

[13] Rivero Belenchón I, Congregado Ruíz CB, Gómez Ciriza G, Gómez Dos Santos V, Rivas González JA, Gálvez García C, González Gordaliza MC, Osmán García I, Conde Sánchez JM, Burgos Revilla FJ and Medina López RA.

How to obtain a 3D printed model of renal cell carcinoma (RCC) with venous tumor thrombus extension (VTE) for surgical simulation (phase I NCT03738488). Updates Surg 2020; 72: 1237-1246.
[14] Gillies RJ and Schabath MB. Radiomics improves cancer screening and early detection. Cancer Epidemiol Biomarkers Prev 2020; 29: 2556-2567.
[15] Shi Z, Traverso A, van Soest J, Dekker A and Wee L. Technical note: ontology-guided radiomics analysis workflow (O-RAW). Med Phys 2019; 46: 5677-5684.
[16] Juusola L, Vanhamäki H, Viljanen A and Smirnov M. Induced currents due to 3D ground conductivity play a major role in the interpretation of geomagnetic variations. Ann Geophys 2020; 38: 983-998.
[17] Addison PS. Introduction to redundancy rules: the continuous wavelet transform comes of age. Philos Trans A Math Phys Eng Sci 2018; 376: 20170258.
[18] Bray F, Ferlay J, Soerjomataram I, Siegel RL, Torre LA and Jemal A. Global cancer statistics 2018: GLOBOCAN estimates of incidence and mortality worldwide for 36 cancers in 185 countries. CA Cancer J Clin 2018; 68: 394-424.
[19] Dogan B, Canda AE, Akbulut Z and Balbay MD. Re: histological subtype is an independent predictor of outcome for patients with renal cell carcinoma: B. C. Leibovich, C. M. Lohse, P. L. Crispen, S. A. Boorjian, R. H. Thompson, M. L. Blute and J. C. Cheville J Urol 2010; 183: 1309-1316. J Urol 2010; 184: 2211; author reply 2211-2.
[20] Pei X, Wang P, Ren JF, Ren JL, Yin XP, Fan SM, Xing LH and Zhou H. Differentiation of high and low grade renal clear cell carcinoma using imaging histology model. J Clin Radiol 2020; 39: 523-527.
[21] Bektas CT, Kocak B, Yardimci AH, Turkcanoglu MH, Yucetas U, Koca SB, Erdim C and Kilickesmez O. Clear cell renal cell carcinoma: machine learning-based quantitative computed tomography texture analysis for prediction of Fuhrman nuclear grade. Eur Radiol 2019; 29: 1153-1163.
[22] Delahunt B, Sika-Paotonu D, Bethwaite PB, William Jordan T, Magi-Galluzzi C, Zhou M, Samaratunga H and Srigley JR. Grading of clear cell renal cell carcinoma should be based on nucleolar prominence. Am J Surg Pathol 2011; 35: 1134-1139.
[23] Moch H, Cubilla AL, Humphrey PA, Reuter VE and Ulbright TM. The 2016 WHO classification of tumours of the urinary system and male genital organs-part A: renal, penile, and testicular tumours. Eur Urol 2016; 70: 93-105.
[24] Delahunt B, Eble JN, Egevad L and Samaratunga H. Grading of renal cell carcinoma. Histopathology 2019; 74: 4-17.
[25] Lubner MG, Smith AD, Sandrasegaran K, Sahani DV and Pickhardt PJ. CT texture analysis: definitions, applications, biologic correlates, and challenges. Radiographics 2017; 37: 1483-1503.
[26] Gillies RJ, Kinahan PE and Hricak H. Radiomics: images are more than pictures, they are data. Radiology 2016; 278: 563-577.
[27] Ganeshan B and Miles KA. Quantifying tumour heterogeneity with CT. Cancer Imaging 2013; 13: 140-149.
[28] Ding J, Xing Z, Jiang Z, Chen J, Pan L, Qiu J and Xing W. CT-based radiomic model predicts high grade of clear cell renal cell carcinoma. Eur J Radiol 2018; 103: 51-56.
[29] Shafiq-Ul-Hassan M, Zhang GG, Latifi K, Ullah G, Hunt DC, Balagurunathan Y, Abdalah MA, Schabath MB, Goldgof DG, Mackin D, Court LE, Gillies RJ and Moros EG. Intrinsic dependencies of CT radiomic features on voxel size and number of gray levels. Med Phys 2017; 44: 1050-1062.